Observation of *d*-band narrowing near copper and nickel surfaces by means of angle-resolved x-ray photoelectron spectroscopy

M. Mehta and C. S. Fadley
Department of Chemistry, University of Hawaii, Honolulu, Hawaii 96822
(Received 17 April 1979)

Angle-resolved x-ray photoelectron spectroscopy has been utilized to determine the full widths at half maximum intensity (FWHM's) and the second moments of the *d* bands of Cu and Ni with variable surface sensitivity. At grazing emission for which the mean excitation depth corresponds to only about 1–2 atomic layers, unambiguous decreases of ~10–12% in the FWHM's and ~18–20% in the second moments are observed relative to the bulk-sensitive values obtained for high-angle emission. These decreases are caused by the reduced coordination number at the surface and are consistent with quantitative predictions based on several recent theoretical studies. The experimental data are compared with theoretical spectra obtained from tight-binding densities of states calculated by Kleinman *et al.* for each atomic layer in a thin metal film. Allowance is made for inelastic scattering of photoelectrons, the refraction of electrons at the surface, and the instrumental resolution. Good agreement is obtained with respect to both the degree of *d*-level narrowing and the changes in fine structure with electron-emission angle. The presence of approximately $\frac{1}{2}$ monolayer of adsorbed oxygen is however found to have no significant effect on the surface *d*-band widths.

I. INTRODUCTION

The development of surface-sensitive experimental techniques such as ion neutralization spectroscopy (INS), photoelectron spectroscopy, and field-emission spectroscopy has stimulated interest in the surface properties of transition metals. One quantity of considerable interest is the electronic density of states (DOS) at the surface. A knowledge of this is important for the understanding of many surface-related physical phenomena such as chemisorption, magnetism near surfaces, and electron tunneling. In recent years, there have been several theoretical investigations of the surface density of states of transition metals.[1–11] These studies predict marked changes in the surface DOS associated with the *d*-orbital-derived levels as compared to the bulk *d*-band DOS. For example, tight-binding linear combination of atomic orbitals (LCAO) calculations by Kleinman *et al.* of the energy bands and the planar densities of states (PDS) for thin Cu,[6] Ni,[7] and Fe,[8] films with various low-index faces exposed indicate that the surface PDS is considerably narrower than the interior PDS's. This is illustrated in Fig. 1 where the planar densities of states for a 47-layer Cu(110) film are presented. Gurman[10] has calculated the *d*-band DOS for Cu(100) films of varying thicknesses and compared them to the bulk DOS. The most notable feature in his calculations is that the *d*-band widths for the one- or two-layer cases are considerably smaller than the bulk value. Also, by the time the film thickness has reached four layers this narrowing effect has virtually disappeared, in agreement with the PDS results of Kleinman *et al.* in Fig. 1. More recently, fully self-consistent calculations have been performed for a Cu(100) monolayer[9] and for Cu(100) films of varying thicknesses.[5] These also indicate that the local density of states varies rapidly in the surface region.

This predicted *d*-band narrowing can be understood in terms of the lowered coordination of the atoms at the surface. Cyrot-Lackmann *et al.*[4,11] have shown that, in the nearest-neighbor tight-binding approximation, the second moment μ of the density-of-states function $\rho(E)$ is proportional to the number of nearest neighbors Z. The mean energy $\bar{E}$ and the second moment μ of $\rho(E)$ are defined as

$$\bar{E} = \left(\int \rho(E) E \, dE / \int \rho(E) dE \right) , \tag{1}$$

$$\mu = \left(\int \rho(E) (E - \bar{E})^2 \, dE / \int \rho(E) dE \right) . \tag{2}$$

Thus the second moment represents the square of the rms bandwidth. The FWHM of the *d*-band peak for transition metals is thus predicted to be approximately proportional to $Z^{1/2}$. For fcc metals, $Z = 8$, 7, and 9, respectively, for the (100), (110), and (111) surfaces. This can be compared to $Z = 12$ in the bulk. Thus reductions of approximately 18.4%, 23.6%, and 13.4% in the *d*-band FWHM are predicted for these three surfaces. Since the effects of the reduced coordination number are mainly operative in the first atomic layer or two, experimental observa-

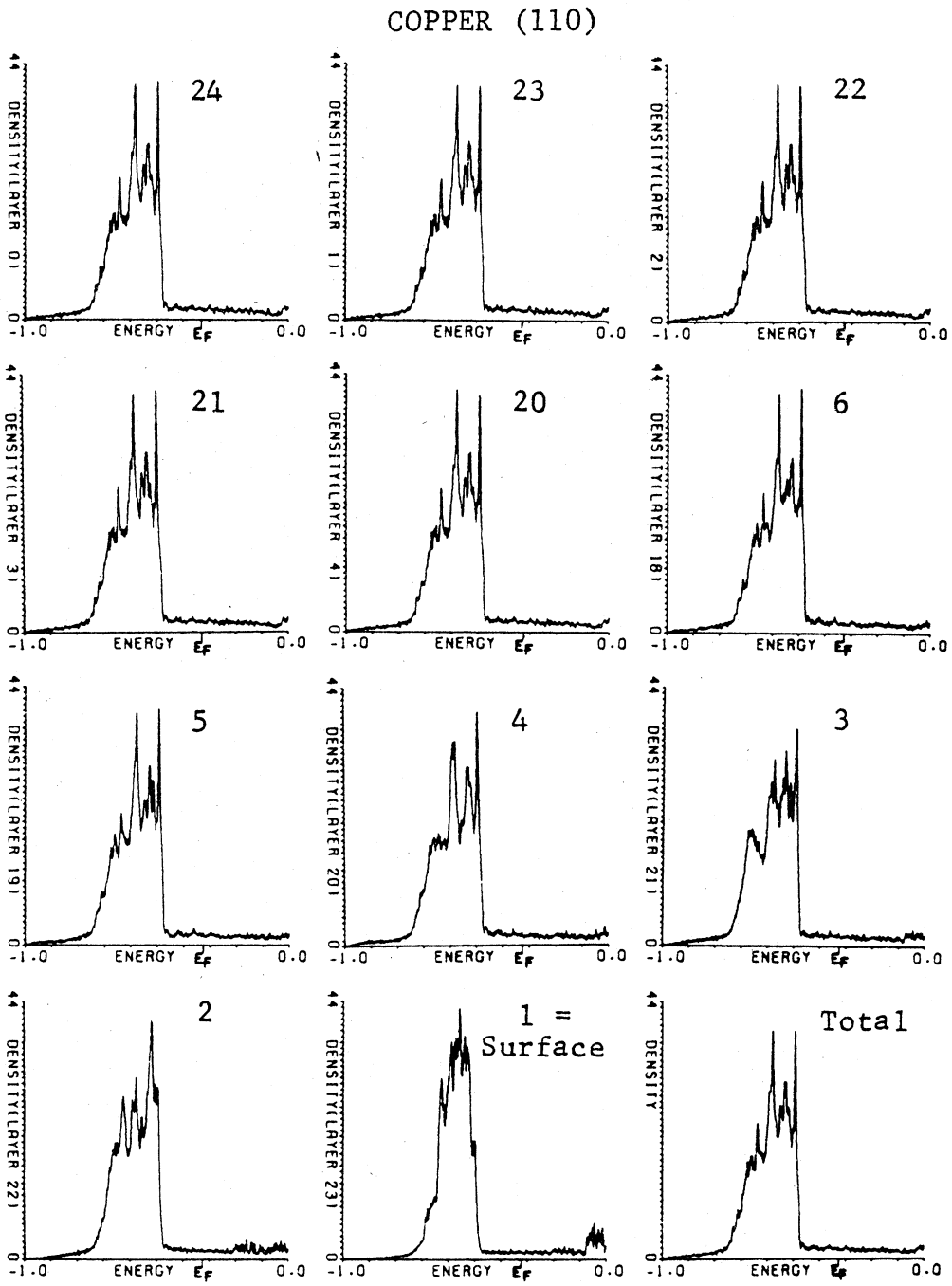

FIG. 1. Planar and total densities of states (in units of $2e$/atom Ry) for a 47-layer Cu (110) film. Layer 1 is the surface layer and 24 is the central layer (From Sohn *et al.*, Ref. 6).

tion of the reduction in either the FWHM or the second moment would require a very surface-sensitive technique. This is also apparent from the planar densities of states of Kleinman *et al.* (cf. Fig. 1) where it can be seen that at the third or fourth layer below the surface the PDS begins to look very much like that of the central layer (that is, the bulk DOS).

As we have first demonstrated in a recent study on Cu,[12] angle-resolved x-ray photoelectron spectroscopy (XPS) can be utilized to detect such differences in the surface and bulk DOS because the surface sensi-

tivity can be enhanced by lowering the electron emission angle with respect to the surface,[13] which will be denoted by θ. Thus, for the example of a grazing 5° emission angle, the average depth of XPS valence emission from Cu is only ~2 layers, as compared to a mean depth of ~10 layers for normal emission ($\theta = 90°$). Therefore, data obtained at grazing emission correspond to a highly surface-sensitive situation while at higher-θ values essentially bulk properties are sampled. For the case of clean polycrystalline Cu, the d-band FWHM has been found to decrease from ~2.5 eV for high-electron emission angle (40°) to ~2.2 eV for grazing emission angle (5°).[12] These small decreases in FWHM have also been shown to be consistent with tight-binding theoretical calculations.[12] Such qualitative d-band narrowing has also been suggested in a few other photoemission[14–17] and INS[18] studies. However, no quantitative correlations between experiment and theory have been attempted in this prior work.

In this paper, we investigate such d-band narrowing effects in greater detail for both Cu and Ni. Experimental valence-band spectra are presented over a range of electron exit angles and are compared with theoretical calculations based upon tight-binding planar densities of states with an allowance for inelastic attentuation and electron-refraction effects at the surface. The angular variations in experimental and theoretical FWHM values and second moments are considered. We have also attempted to determine the effects of an adsorbed oxygen overlayer on the d-band electron structure at the surface.

II. EXPERIMENTAL

Experimental spectra were obtained with a Hewlett-Packard 5950A photoelectron spectrometer that had been specially modified so as to permit automated angular distribution studies under ultrahigh vacuum conditions.[13] Variation of the electron emission angle θ was effected by rotating the specimen about an axis that lay in its surface and was also perpendicular to the plane containing the x-ray and electron propagation directions. The angle θ is measured with respect to the surface, so that $\theta = 90°$ corresponds to exit perpendicular to the surface. Monochromatized Al $K\alpha$ radiation at 1487 eV was used for excitation. The dispersion-compensating electron and x-ray optics of the spectrometer yielded a minimum FWHM for Au $4f_{7/2}$ of 0.8 eV in the angle range considered. Resolution in this spectrometer is, however, a function of the polar emission angle θ, as discussed in detail by Baird and Fadley.[19] The pressure inside the spectrometer chamber was in the range 5×10^{-11}–1×10^{-10} Torr during all measurements. Cleanliness of the sample surfaces was checked by periodic *in situ* monitoring of the C-1s and O-1s peaks. All valence spectra were corrected for inelastic scattering backgrounds and instrumental resolution changes with θ. These correction procedures will be discussed in detail for the example of Cu.

III. RESULTS AND DISCUSSION

A. Copper

Polycrystalline copper specimens were prepared by *in situ* vapor depositions of 99.999% purity Cu on smooth glass substrates (Corning 7059). The polycrystalline character was verified by subsequent examination by Laue back reflection. The films were deposited in less than 30 sec with operating pressures during deposition in the 10^{-8}-Torr range. The pressure fell to $\lesssim 6 \times 10^{-10}$ Torr within two minutes after deposition. Base pressures during accumulation of spectra were $\sim 5 \times 10^{-11}$–1×10^{-10} Torr. The deposited sample surfaces were cleaned by argon-ion bombardment until the only impurity noted was a very low level of oxygen corresponding to a fractional monolayer coverage from 2–6% as determined from the relative intensities of the O-1s and Cu-3s peaks; no increase in this level was observed during the duration of the measurements. Based upon atomic photoelectric cross sections for Al $K\alpha$,[20] such oxygen levels should produce only ~0.5–2% of the valence spectral intensity originating in the outermost atomic layer of the surface, and so should be negligible in this study. Spectra were obtained for the valence levels and the Cu-$2p_{3/2}$ and Cu-3p core peaks with binding energies of 931 and 74 eV, respectively, over the θ range from 5° to 40°.

The valence spectra were corrected for the inelastically scattered electrons by assuming an inelastic background at each kinetic energy that is proportional to the integrated no-loss intensity at higher energies.[12,21] In support of this assumption, an analysis of Cu-3p core spectra indicated inelastic-loss tails that were very nearly flat in energy over the entire angle range studied, although there was a slight slope of ~−4%/eV in the lowest angle spectrum at 5° (the negative sign indicates a decrease in loss intensity with increasing distance from the no-loss peak). Additional calculations performed for a linearly sloping background with empirically optimized choices of the slope did not significantly alter either the corrected spectral shapes or d-band widths. Thus the assumption of a constant loss probability with energy corresponding to an asymptotic zero-slope background was considered quite reasonable and was used in all data analyses. Raw data and background-corrected valence-band spectra are presented in Fig. 2 for $\theta = 40$, 20, and 5°. An additional correction of importance is that associated with instrumental reso-

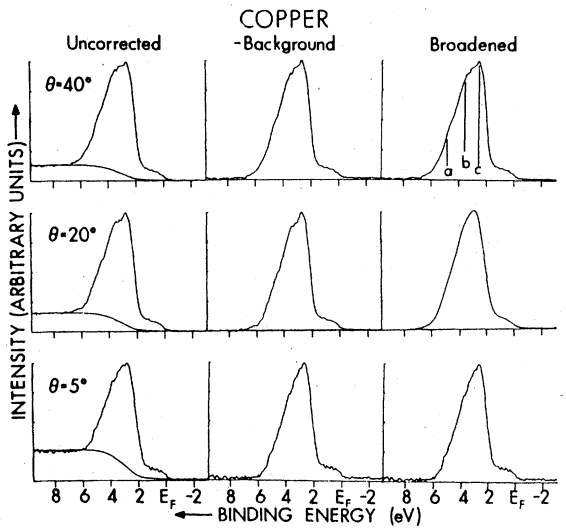

FIG. 2. X-ray photoemission spectra of the valence-band region of polycrystalline copper at three electron exit angles. 90° is normal exit. In the first column, the raw data appear, together with an iteratively determined inelastic background. In the second column, the inelastic background has been subtracted, and in the third column, the corrected spectra have been broadened so as to result in a constant effective instrumental resolution at all angles.

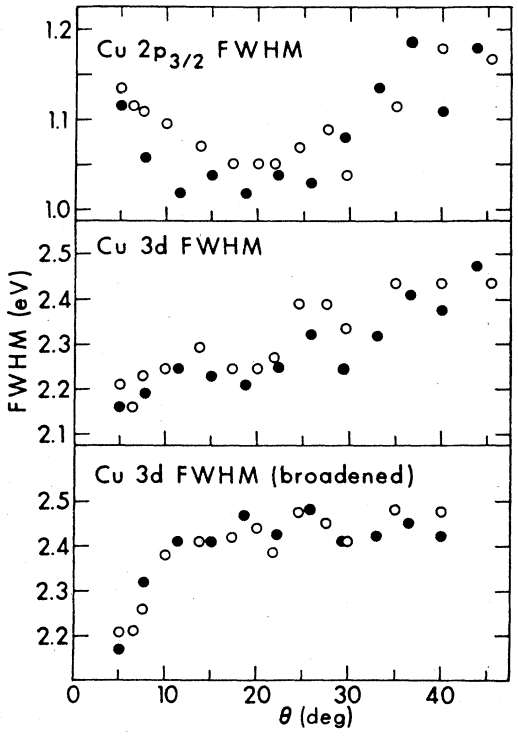

FIG. 3. Angular dependence of the full width at half maximum intensity of the experimental Cu-$2p_{3/2}$ and Cu d-band spectra. The FWHM have been derived from polycrystalline spectra corrected for inelastic scattering effects (cf. Fig. 1). In the bottom panel the d-band FWHM have also been corrected for instrumental resolution changes by appropriate broadening. The open and closed data points represent two different sets of measurements.

lution changes with θ.[19] Figure 3 shows the angular variation in FWHM derived from background-corrected spectra for the Cu-$2p_{3/2}$ core levels and the Cu valence bands. The Cu-$2p_{3/2}$ FWHM passes through a minimum at $\theta \approx 20°$ and increases by about 0.2 eV at either $\theta = 5$ or 40°. This is fully consistent with the changes in instrumental resolution expected for the dispersion-compensating spectrometer utilized in this study and a similar variation in the C-1s FWHM for graphite has been observed by Baird and Fadley.[19] The FWHM's of the Cu valence bands, however, continue to decrease for $\theta < 20°$, and between $\theta = 40°$ and $\theta = 5°$ (angles for which the instrumental resolution is nearly identical, as can be seen from the core level FWHM's) a decrease of $\sim$11% is observed. Although corrections for instrumental resolution changes with θ are not critical to determining the overall d-band width changes between high- and low-angle because this can be done between angles with the same instrumental resolution, we have allowed for such changes by broadening the spectra at all angles to a constant resolution consistent with the maximum over the angle range of interest. The broadening functions were determined from an analysis of the Cu-$2p_{3/2}$ core spectra. The Cu-$2p_{3/2}$ spectrum at each angle was broadened by a Gaussian function of such a width as to yield the same spectral shape and width as that of the maximum width spectrum in the 5–40° angle range studied. Each broadening function so derived was then applied to the corresponding valence spectrum. Such fully corrected valence-band spectra are presented in Fig. 2, and these corrected spectra also show a decrease of $\sim$12% in the FWHM at low θ as shown in the bottom panel of Fig. 3. It can also be seen in Fig. 2 that there are subtle changes in peak shapes with angle and that there is a general sharpening of the d-band peak at lower θ values.

Theoretical calculations of the expected band narrowing have been performed using the tight-binding layer densities of states calculated by Kleinman and Caruthers *et al.*[6] within an extended Hückel approximation. In order to make the closest possible comparison with the XPS data, the effects of no-loss signal attenuation due to inelastic scattering and electron refraction at the surface have been included in our model theoretical calculations. However, any matrix element modulations across the valence bands are neglected, as are any changes in valence spectra with emission direction due to specimen single-crystal character.[15] Thus, if $\rho(E)_j$ represents the density of states of layer j, z_j its depth below the surface, Λ_e the inelastic electron attenuation length, and θ' the inter-

TABLE I. Calculations of internal propagation angle θ' and the effective sampling depth $\Lambda_e \sin\theta'$ at various external electron exit angles θ for emission from Cu valence levels with Al $K\alpha$ excitation (1487 eV). For comparison, the atomic layer spacings for different surfaces are also given.

θ(observed)	θ'(internal)	$\Lambda_e \sin\theta'$(Å)
5°	7.4°	1.9
10°	11.4°	3.0
20°	20.7°	5.3
30°	30.5°	7.6
40°	40.3°	9.7
50°	50.2°	11.5
70°	70.1°	14.1
90°	90.0°	15.0

$d_{001} = 1.81$ Å, $d_{011} = 1.28$ Å, $d_{111} = 2.09$ Å.

nal angle of propagation corresponding to an external exit angle θ, the simplest prediction of angular-dependent XPS spectra within the three-step model is given by

$$I(E) = \sum_{j=1}^{\infty} \rho(E)_j \exp(-z_j/\Lambda_e \sin\theta') \quad . \tag{3}$$

The internal angle of propagation θ' and the mean depth for no-loss emission (which will be given in this model by $\Lambda_e \sin\theta'$) are presented for several θ values in Table I and it is clear that at the lowest angle of 5°, the first surface layer or two should dominate the spectra. The difference between θ' and the external angle θ also demonstrates that electron refraction is a significant correction for the lowest angles studied here. For these calculations, an inner potential of 13.8 eV [the sum of the theoretical 8.98-eV Fermi energy[22] and the 4.8-eV work function for the copper (100) face[6]] and an inelastic attenuation length of 15 Å [23] have been used. The results of such calculations are shown in the first column in Figs. 4, 5, and 6 for the (100), (110), and (111) faces of Cu and the three electron exit angles of 40°, 20°, and 5°. In the second column, the theoretical

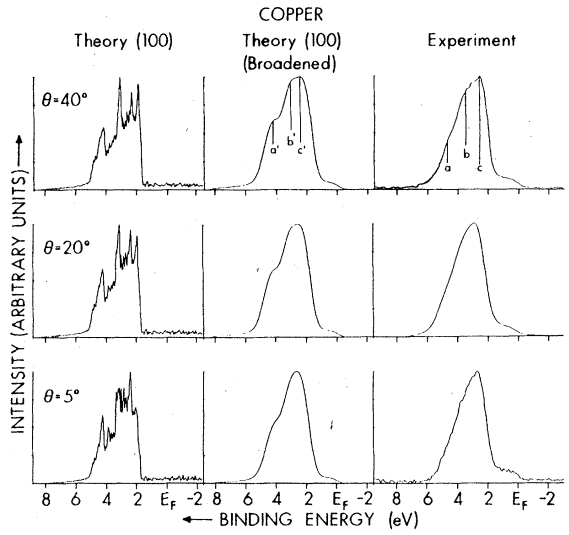

FIG. 4. Theoretical XPS spectra for a Cu(100) film calculated for three different electron exit angles with Eq. (3). In the second column, the theoretical curves are broadened by the experimental resolution. Corrected experimental data for polycrystalline copper are presented for comparison in column three.

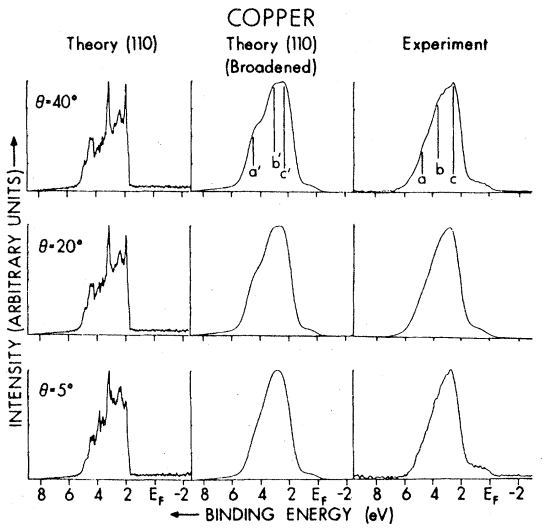

FIG. 5. Analogous to Fig. 4 but for a Cu(110) film.

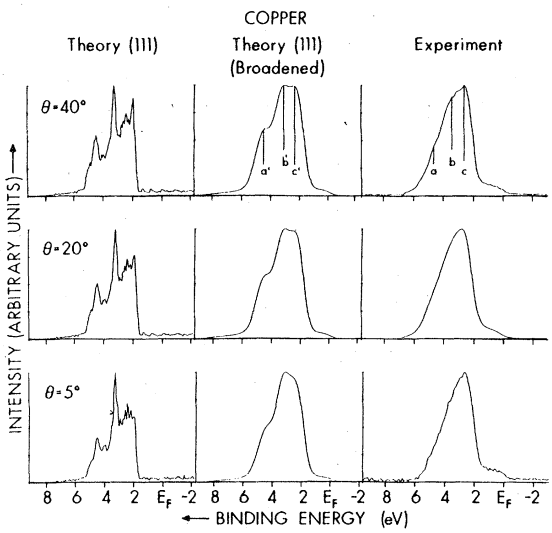

FIG. 6. Analogous to Fig. 4 but for a Cu(111) film.

curves have been broadened by a Gaussian of 0.80-eV FWHM to simulate instrumental and natural lifetime contributions. In the third column, the fully corrected experimental spectra are shown. There is generally good agreement between the broadened theoretical spectra and the experimental data with respect to changes in both peak shapes and peak widths. Changes in peak shapes can be detected from the relative intensities of the features a, b, and c in the experimental data and the corresponding features a', b', and c' in the theoretical spectra. It is also apparent that the theoretical spectra for all three faces are very similar, with the only notable difference being that for (111), the b' intensity is higher than the c' intensity.

The angular dependence of the experimental and theoretical Cu d-band FWHM is presented in Fig. 7. There is generally good agreement as to the form of the curves and the approximate degree of d-band narrowing noted, with theory predicting a 17.5% change between 40° and 5° in comparison to the experimentally observed 11.8%. The mean theoretical narrowing of 17.5% is also in good agreement with the average narrowing predicted for the three faces from the change in coordination number at the surface; this average over (100), (110), and (111) is 18.5%. These calculations also indicate that the FWHM changes only very slightly (~1.5%) over the higher 40–90° angle range, so that the width changes discussed here are essentially the complete range expected.

The discrepancy between experiment and theory could arise from several sources:

(i) The presence of surface roughness which will, in general, cause the macroscopic angle of detection to be less than the true microscopic angle of emission.[13] Such roughness effects would also explain the slower onset of the decrease in FWHM with decreasing θ for experiment. Scanning electron micrographs of the specimen surfaces at a magnification of 56 000 showed very little surface roughness, but some undulations were present with ~500 Å periods and undetermined heights.

(ii) *Elastic* electron scattering, which may tend to deflect electrons initially excited at higher θ' values into lower angles at some point during their escape from the specimen.

(iii) The various approximations inherent in the theoretical model used here, including neglect of matrix-element and single-crystal effects.

(iv) Surface relaxation (that is, a layer spacing near the surface that is different from the layer spacing in the bulk), which might influence the d-band width at the surface. It has recently been pointed out[24] that even a slight compression of only a few percent in the first interplanar spacing could cancel the effect of reduced coordination number on the d-band width. However, theoretical calculations of the relaxation near transition-metal surfaces[25] indicate that for metals with almost empty or filled d bands there is essentially no surface relaxation. Also, comparisons of calculated and experimental low-energy electron

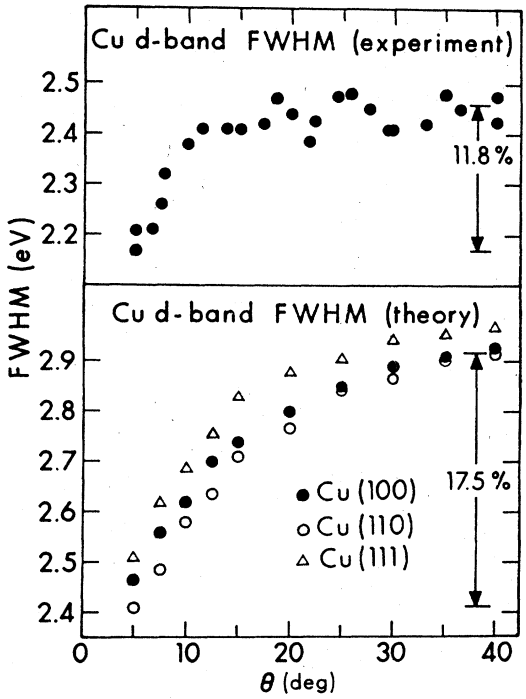

FIG. 7. Experimental and theoretical variation of the copper d-band FWHM with θ. The experimental FWHM have been derived from polycrystalline spectra corrected for inelastic scattering and instrumental resolution changes. Theoretical FWHM values have been determined for the three low-index surfaces (100), (110), and (111) from broadened, weighted densities of states as in Figs. 4–6.

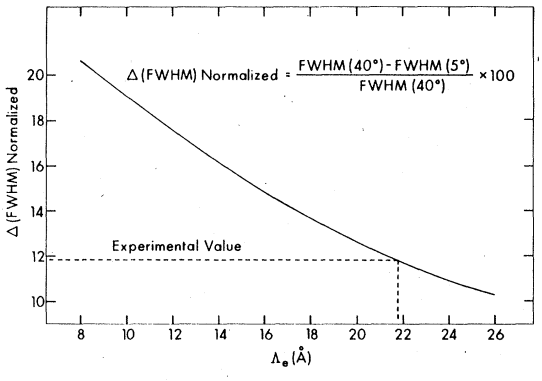

FIG. 8. Effect of changing the electron attenuation length Λ_e on the d-band narrowing as calculated with Eq. (3). The percentage change in the FWHM between $\theta = 40°$ and $\theta = 5°$ is plotted as a function of Λ_e. Calculations are for a Cu(100) surface.

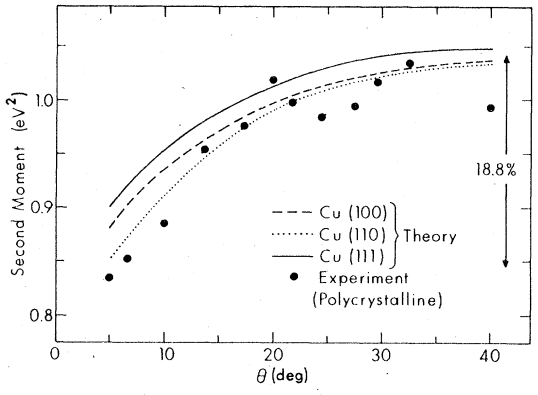

FIG. 9. Experimental and theoretical angular dependence of the Cu d-band second moment.

diffraction (LEED) intensity profiles for Cu(100) indicate[26] that the best agreement is obtained when the upper-layer spacing is equal to the bulk spacing. For Cu(111) by contrast,[26] there may be a slight contraction of ~5% in the surface-layer spacing. Thus, a small amount of surface relaxation cannot be ruled out and this could further explain the discrepancy between theory and experiment.

(v) The value chosen for Λ_e may be too small. Thus theory may overestimate the contribution from the surface layer, thereby producing an anomalously large narrowing in the calculations. Such effects are indicated in Fig. 8 where the percentage decrease in the d-band FWHM between $\theta=40°$ and $\theta=5°$ is plotted as a function of the Λ_e value chosen. It can be seen that a relatively small increase of Λ_e from 15 to 22 Å yields the observed 12% decrease.

(vi) The use of the theoretically more correct second moment as a width indicator [cf. Eq. (2)] also is found to improve agreement between experiment and theory, although isolating the "d-band" intensity between approximately 1.0 and 5.5 eV for computing μ cannot be done in a fully unambiguous way. The second moment was calculated over the d-band peak by excluding the s, p intensity occurring at ~0–1 eV and ~5.5–8 eV, with cutoff points chosen to lie at the points of maximum curvature in the theoretical or experimental spectra. A summary of these results is presented in Fig. 9. Very good agreement is obtained between experiment and theory, with changes between 40° and 5° of ~19% in both the experimental data and the theoretical calculations for all three low-index faces.

B. Nickel

A nickel sample was prepared by mechanically polishing 99.999% pure polycrystalline Ni to a mirror finish with SiC paper, diamond paste, and finally CeO of $\frac{1}{4}$-micron diameter. Before loading into the vacuum system, the specimen was etched briefly in a dilute $HF\text{-}HNO_3$ mixture to reduce surface roughness. It was then cleaned *in situ* by alternate cycles of argon-ion bombardment ($P_{Ar}=5\times10^{-5}$ Torr, $V_{ion}=700$ V, $I_{ion}=7$ μA, for a time of 15 mins) and annealing (600 °C, 1 h). Small amounts of C and S always diffused to the surface and the cleaning treatment had to be repeated periodically to maintain an acceptable surface. However, the fractional coverages of C and S on the surface were at no time greater than 10% of a monolayer, levels that should yield negligible contributions to the valence spectral intensities. Ni-$2p_{3/2}$ (binding energy of 854 eV) and Ni valence-band spectra were obtained for θ values ranging from 5° to 40°. Counting times were shorter than those for Cu because the specimen had to be taken out of the main spectrometer chamber at about every 12 hours for cleaning. To minimize errors due to poor statistics, four sets of spectra were obtained and summed.

Raw spectra for the Ni-$2p_{3/2}$ and the Ni-$3d$ peaks are presented in Fig. 10. The origin of the broad structures about 6 eV to the high-binding energy side of both the $3d$ peak and the $2p$ core peak is uncertain, although they have been observed in many prior photoemission studies.[27–33] The data shown here make it clear that these broad peaks are essentially identical in both valence and core emission, and therefore make it unlikely that they represent valence-specific effects. The explanation of these features will not concern us here, but their contributions to spectral intensity near the d-band peaks must be taken into account in the background subtraction procedure. The inelastic scattering background was calculated over the relatively flat portions extending about 6 eV on either side of the d-band peak as shown in Fig. 10. After correcting for inelastic scattering, the spectra were broadened in a self-consistent way to allow for instrumental resolution

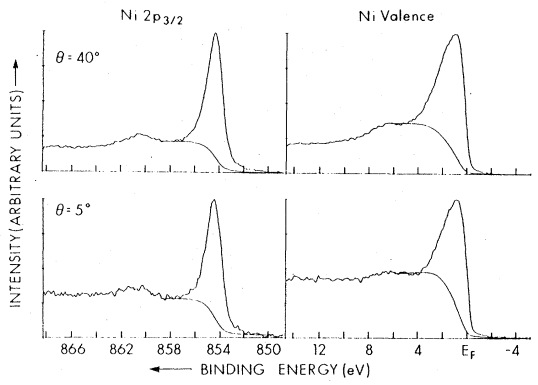

FIG. 10. Ni-$2p$ and Ni valence-band XPS spectra at $\theta=40°$ and $\theta=5°$. Note the broad weak structures centered at about 6 eV to the high-binding energy side of the main peaks.

changes, by means of the same procedure discussed for copper. Figure 11 shows the uncorrected and corrected Ni valence-band spectra for three electron exit angles. Although less fine structure is noted in the experimental Ni valence spectra than in those of Cu, the same general sharpening of the principal peak at ~1 eV below E_F is noted between 40° and 5° (cf. Fig. 2). The Ni-$2p_{3/2}$ and Ni d-band FWHM values derived from the corrected spectra are further presented in Fig. 12. Between the high and the low angle, the d-band peak is found to narrow in width by ~11%.

Theoretical calculations of the band-narrowing effect were performed with the same method described for copper. These calculations were based upon planar densities of states calculated for a 35-layer ferromagnetic Ni (100) film by Kleinman *et al.*[7] The planar densities of states for spin-up and spin-down electrons with an exchange splitting of ~0.4 eV were added to give the total planar densities of states. The inner potential assumed was 13.9 eV. An electron attenuation length of 15 Å was used. The results of these calculations are presented in Fig. 13 together with the experimental spectra. Definite changes in peak shapes and widths with angle are observed for these theoretical curves. For example, the shoulder b' at ~1.8 eV below E_F that is almost as strong as the dominant peak c' at 40° almost disappears at 5°, and the shoulder a' at ~3.5 eV below E_F also becomes much less pronounced at this lower angle. The theoretical curves are in this respect semiquantitatively consistent with the experimental data, although there is much less structure in the experimental curves. The FWHM values derived from the theoretical peaks decrease from ~3.7 eV at 40° to ~2.6 eV at 5°. Thus a narrowing of ~30% that is much higher than the 11% effect noted experimentally is predicted. The various reasons given in the prior Cu discussion could also account for this discrepancy for Ni. The specimen surface was examined by scanning electron microscopy at a magnification of 64,000 and found to exhibit no significant roughness contours. Thus roughness is not likely to be a more significant factor for Ni than for Cu. Surface atomic

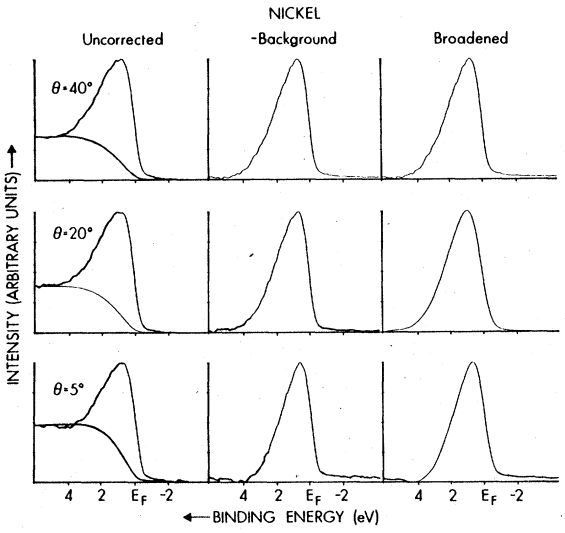

FIG. 11. Analogous to Fig. 2 but for a polycrystalline Ni specimen.

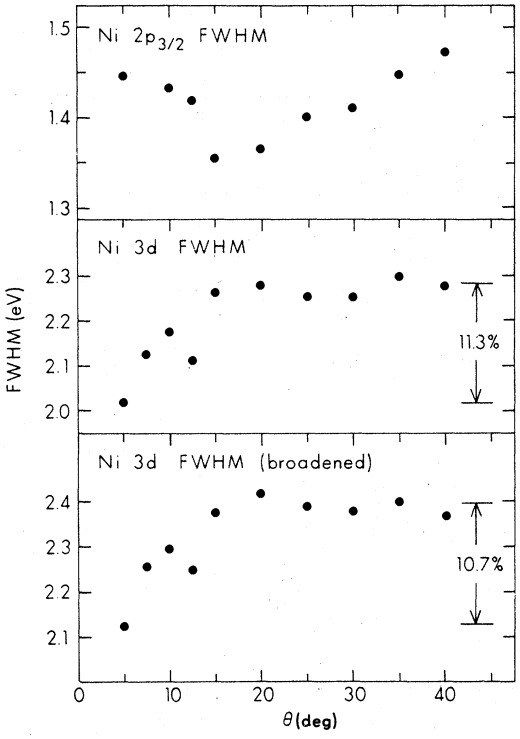

FIG. 12. Analogous to Fig. 3 but for Ni.

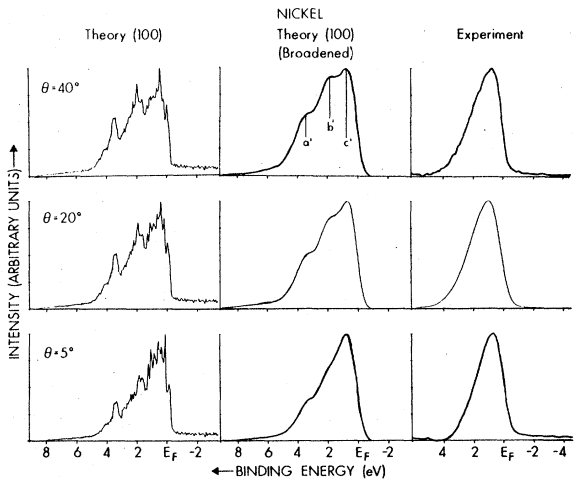

FIG. 13. Analogous to Fig. 4 but for Ni.

geometry relaxation, however, may be more significant for Ni. Demuth *et al.*[34] have performed a LEED analysis for the low-index planes of Ni and they report that the upper-layer spacing for the (110) plane is contracted by ~5% and also that the (111) plane is possibly contracted by ~2%, while the (100) surface is expanded by ~2% relative to the bulk. Also, since the theoretical spectra for Ni have a considerable amount of visible structure, the FWHM may not be as good a width indicator and a measure in terms of the second moment might be better. Second-moment calculations for experiment and theory are thus shown in Fig. 14. These calculations have been performed over the *d*-band peak only to avoid any spurious effects due to both the *s*, *p* bands and the extra structure that is found in the Ni spectra at ~6 eV below E_F (cf. Fig. 10). The second-moment calculations indicate a band narrowing of about the same order for both theory and experiment, with a difference between 40° and 5° of 11% in the former and 21% in the latter. Thus, both for copper and nickel, the use of the second moment yields better agreement between experiment and theory. Also, the fact that theory and experiment for Ni disagree in opposite directions when FWHM and second-moment values are considered suggests that no single error that is consistently in the same direction is present in both analyses. It should finally be noted that the absolute experimental *d*-band widths and second moments for all angles are much smaller than the theoretical DOS estimates. This is consistent with prior photoemission data.[27,28,33,35]

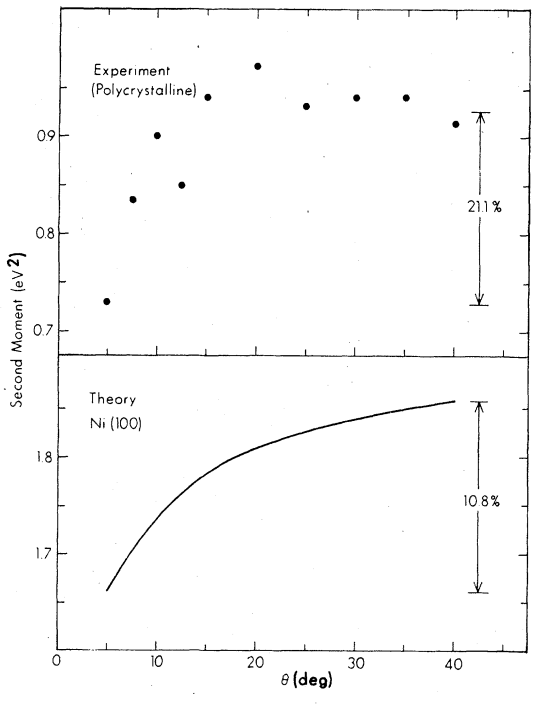

FIG. 14. Experimental and theoretical variation of the Ni *d*-band second moment. Experimental data is for a polycrystalline specimen and theoretical calculations for a Ni(100) surface.

It should also be noted that our analysis assumes that the valence-band spectra are closely related to the one-electron density of states. Since the core-hole spectra are influenced by many-body final-state effects, it has been argued by several authors[33,35,36] that a one-electron approach is not adequate for describing the photoemission spectra of the valence bands. However, recent angle-resolved photoemission measurements on Ni single crystals[37] have shown that many-body effects play only a minor role in determining the energy distribution curves.

IV. EFFECTS OF ADSORBED OXYGEN

It is also of interest to determine whether surface *d*-band narrowing is affected by the presence of an adsorbate. If there is a strong interaction between the metal and the adsorbate, it might be expected that, for a saturation coverage, the surface atoms of the metal would attain their full complement of nearest neighbors and thus perhaps become more bulklike in character. Under these circumstances, the *d*-band narrowing which arises from the reduced coordination number at the surface might be expected to disappear or at least be reduced. This effect was investigated for both polycrystalline Ni and Cu. For Ni, oxygen exposures of 10 L were used; prior experiments on Ni single crystals indicate that such exposures on a (100) surface lead to the formation of an ordered $c(2\times2)$ structure (0.5 monolayer coverage),[38,39] an ordered 2×2 structure (0.25 monolayer coverage) on a (111) surface[40] and a 0.67 monolayer coverage on a (110) surface.[41] For the polycrystalline specimen used in this study, a 10-L exposure resulted in a 0.8 monolayer coverage as estimated from the O1*s* to Ni3*s* ratio and this coverage is thus consistent with the single-crystal work. The FWHM's for the *d*-band spectra obtained without and with an oxygen overlayer are compared in Fig. 15 and they indicate that essentially the same degree of band narrowing persists after oxygen adsorption. Similar experiments performed on Cu specimens with a 1000-L oxygen exposure (corresponding to ~0.3 monolayer coverage) indicated a somewhat reduced band narrowing (7% as compared to 12% observed for the clean surface). Thus these oxygen adsorption studies are not fully conclusive, although the general persistence of band narrowing suggests that the interactions between the oxygen atoms and the metal atoms at the surface may not be strong enough to perturb the band structure. Alternatively, the metallic surface-band narrowing might be disappearing, but at the

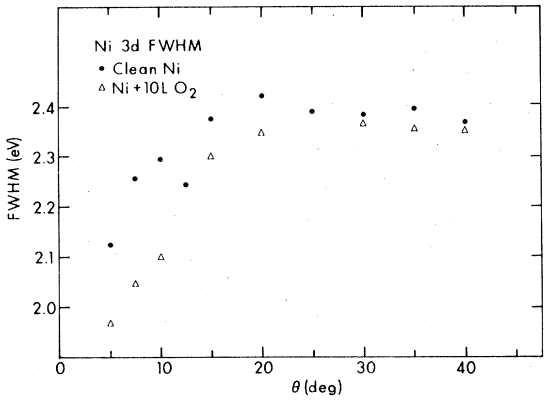

FIG. 15. Variation of the Ni d-band FWHM with θ for a clean and oxygen-exposed Ni surface.

same time, an increase in the upper-layer spacing might affect the widths for the lower, more surface-sensitive angles. LEED structural analyses of an adsorbed oxygen overlayer on surfaces of Cu,[42–45] and Ni,[44–46] single crystals have been performed by several workers. The main thrust of these prior studies has, however, been to examine the positions of the adsorbed atoms. Unfortunately, there have been notable discrepancies in the results reported by different authors so no unambiguous conclusion is possible concerning the effect of adsorbed oxygen upon the surface-metal layer spacings. However, a LEED analysis of a 1×1 oxygen overlayer on the (001) surface of Fe indicates[47] that the agreement between the experimental and theoretical spectra is much improved if an expansion of $\sim$7.5% between the first- and second-Fe layers is considered than if an unrelaxed substrate is assumed. Thus, it is possible that the presence of adsorbed atoms could cause similar atomic relaxations in other metals as well, thus possibly influencing the degree of d-band narrowing. Finally, the formation of adsorbate-metal bonds could inherently lead to a narrowing of the electronic levels in the d-band region.

V. CONCLUSIONS

Unambiguous changes in both the width and fine structure of the Cu and Ni d-band peaks have thus been observed between high-angle and low-angle x-ray photoemission. The results are summarized in Fig. 16, where the fully corrected spectra are presented for both copper and nickel at electron exit angles of 40° and 5°. The enhanced surface sensitivity occurring at grazing emission suggests that these effects are due to near-surface band-structure alterations caused by reduced coordination number. Theoretical

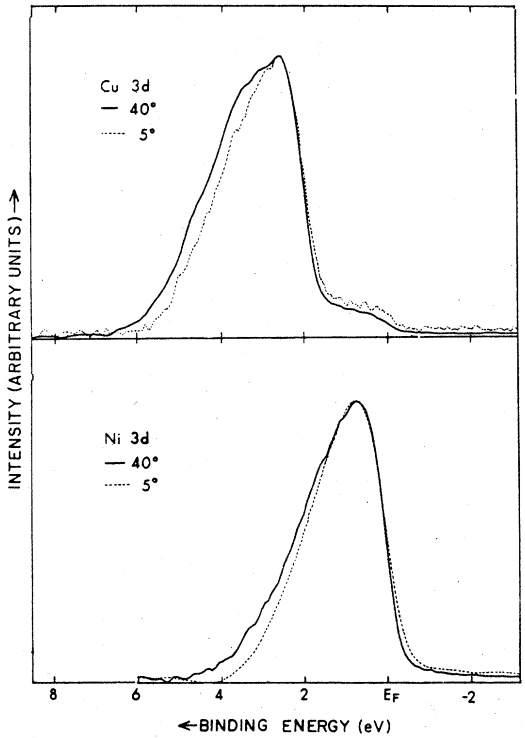

FIG. 16. Fully corrected experimental spectra for the Cu and Ni d bands at electron exit angles of 40° and 5°. The spectra at the two angles are superimposed to emphasize the band narrowing observed at the lower angle.

calculations based upon tight-binding densities of states for various near-surface layers and including inelastic electron attenuation and surface refraction predict all of the observed changes in spectra with angle. Thus, a simple tight-binding model appears capable of describing such effects rather well, although it would be of interest to use layer densities of states calculated for thicker films by means of more self-consistent procedures such as those now being developed by several groups.[5,9,48] Such angular-dependent XPS studies thus should prove useful in further characterizing surface-associated valence-level changes in metals and other materials.

ACKNOWLEDGMENTS

We would like to thank L. Kleinman and D. G. Dempsey for supplying us with the planar densities of states for copper and nickel prior to publication. The support of the NSF (Grant No. CHE76-24506) and the Petroleum Research Fund administered by the American Chemical Society is also gratefully acknowledged.

[1]D. Kalstein and P. Soven, Surf. Sci. 26, 85 (1971).
[2]R. Haydock, V. Heine, M. J. Kelly, and J. B. Pendry, Phys. Rev. Lett. 29, 868 (1972).
[3]R. Haydock and M. J. Kelly, Surf. Sci. 38, 139 (1973).
[4]M. C. Desjonquères and F. Cyrot-Lackmann, Surf. Sci. 53, 429 (1975).
[5]J. G. Gay, J. R. Smith, and F. J. Arlinghaus, Phys. Rev. Lett. 38, 561 (1977).
[6]K. S. Sohn, D. G. Dempsey, L. Kleinman, and E. Caruthers, Phys. Rev. B 13, 1515 (1976); B 14, 3185 (1976); B 14, 3193 (1976); and earlier references therein, and D. G. Dempsey and L. Kleinman (private communication).
[7]D. G. Dempsey, W. R. Grise, and L. Kleinman, Phys. Rev. B 18, 1270 (1978); B 18, 1550 (1978), and L. Kleinman (private communication).
[8]D. G. Dempsey, L. Kleinman, E. Caruthers, Phys. Rev. B 12, 2932 (1975); B 13, 1489 (1976); B 14, 279 (1976).
[9]C. S. Wang and A. J. Freeman, Phys. Rev. B 18, 1714 (1978).
[10]S. J. Gurman, J. Phys. F 5, L194 (1975).
[11]F. Cyrot-Lackman, J. Phys. Chem. Solids 29, 1235 (1968).
[12]M. Mehta and C. S. Fadley, Phys. Rev. Lett. 39, 1569 (1977).
[13]C. S. Fadley, Prog. Solid State Chem. 11, 265 (1976).
[14]J. Stöhr, G. Apai, P. S. Wehner, F. R. McFeeley, and D. A. Shirley, Phys. Rev. B 14, 5144 (1976).
[15]L. F. Wagner, Z. Hussain, C. S. Fadley, and R. J. Baird, Solid State Commun. 21, 453 (1977); L. F. Wagner, Z. Hussain, and C. S. Fadley, Solid State Commun. 21, 257 (1977).
[16]J. C. Fuggle and D. Menzel, Surf. Sci. 53, 21 (1975).
[17]P. H. Citrin and G. K. Wertheim, Phys. Rev. Lett. 41, 1425 (1978).
[18]H. D. Hagstrum and G. E. Becker, Phys. Rev. 159, 572 (1967); J. Chem. Phys. 54, 1015 (1971).
[19]R. J. Baird and C. S. Fadley, J. Electron Spectrosc. 11, 39 (1977).
[20]J. H. Scofield, J. Electron Spectrosc. 8, 129 (1976).
[21]R. Pollak, L. Ley, S. Kowalczyk, and D. A. Shirley, Phys. Rev. Lett. 29, 1088 (1972).
[22]G. A. Burdick, Phys. Rev. 129, 138 (1963).
[23]C. J. Powell, Surf. Sci. 44, 29 (1974); D. R. Penn, J. Electron Spectrosc. 9, 29 (1976).
[24]G. Allan and J. N. Decarpigny, Phys. Lett. A 65, 143 (1978).
[25]G. Allan and M. Lannoo, Surf. Sci. 40, 375 (1973).
[26]G. E. Laramore, Phys. Rev. B 9, 1204 (1974).
[27]D. E. Eastman, J. Phys. (Paris) 32, C1-293 (1971).
[28]L.-G. Petersson, R. Melander, D. P. Spears, and S. B. M. Hagström, Phys. Rev. B 14, 4177 (1976).
[29]R. J. Smith, J. Anderson, J. Hermanson, and G. J. Lapeyre, Solid State Commun. 21, 459 (1977).
[30]K. S. Kim and N. Winograd, Surf. Sci. 43, 625 (1974).
[31]Y. Baer, P.-F. Hedèn, J. Hedman, M. Klasson, C. Nordling, and K. Siegbahn, Physica Scripta 1, 55 (1970).
[32]S. Hüfner and G. K. Wertheim, Phys. Lett. A 51, 299 (1975).
[33]P. C. Kemeny and N. J. Shevchik, Solid State Commun. 17, 255 (1975).
[34]J. E. Demuth, P. M. Marcus, and D. W. Jepsen, Phys. Rev. B 11, 1460 (1975).
[35]S. Hüfner, G. K. Wertheim, and J. H. Wernick, Solid State Commun. 17, 417 (1975).
[36]N. J. Shevchik and C. M. Penchina, J. Phys. F 5, 2008 (1975).
[37]M. Sagurton, D. Leibowitz, and N. J. Shevchik, Solid State Commun. 25, 955 (1978), and D. E. Eastman *et al.* (private communication).
[38]P. H. Holloway and J. B. Hudson, Surf. Sci. 43, 141 (1974).
[39]S. Ohtani, K. Terada, and Y. Murata, Phys. Rev. Lett. 32, 415 (1974).
[40]H. Conrad, G. Ertl, J. Küppers, and E. E. Latta, Surf. Sci. 57, 475 (1976).
[41]J. W. May and L. H. Germer, Surf. Sci. 11, 443 (1968).
[42]L. McDonnell, D. P. Woodruff, and K. A. R. Mitchell, Surf. Sci. 45, 1 (1974).
[43]L. McDonnell and D. P. Woodruff, Surf. Sci. 46, 505 (1974).
[44]C. B. Duke, N. O. Lipari, and G. E. Laramore, J. Vac. Sci. Technol. 11, 180 (1974).
[45]S. Andersson, B. Kasemo, J. B. Pendry, and M. A. VanHove, Phys. Rev. Lett. 31, 595 (1973).
[46]J. E. Demuth, D. W. Jepsen, and P. M. Marcus, Phys. Rev. Lett. 31, 540 (1973).
[47]K. O. Legg, F. P. Jona, D. W. Jepsen, and P. M. Marcus, J. Phys. C 8, L492 (1975).
[48]I. P. Batra and S. Ciraci, Phys. Rev. Lett. 39, 774 (1977).